DOI: http://dx.doi.org/10.15446/ing.investig.v35n3.47386

New digital demodulator with matched filters and curve segmentation techniques for BFSK demodulation: Analytical description

Nuevo demodulador digital con filtros macheados y técnicas de segmentación de curvas para la demodulación de señales BFSK: Descripción analítica

J. Torres[1], F. Hernández[2], and J. Habermann[3]

ABSTRACT

The present article relates, in general, to digital demodulation of Binary Frequency Shift Keying (BFSK). The objective of the present research is to obtain a new processing method for demodulating BFSK-signals in order to reduce hardware complexity in comparison with other methods reported. The solution proposed here makes use of the matched filter theory and curve segmentation algorithms. This paper describes the integration and configuration of a Sampler Correlator and curve segmentation blocks in order to obtain a digital receiver for a proper demodulation of the received signal. The proposed solution is shown to strongly reduce hardware complexity. In this part, a presentation of the proposed solution regarding the analytical expressions is addressed. The paper covers in detail the elements needed for properly configuring the system. In a second article the implementation of the system for FPGA technology and the simulation results in order to validate the overall performance are presented.

Keywords: Matched filters, curve segmentation, digital demodulation, BFSK, FPGA.

RESUMEN

El presente artículo está relacionado con la demodulación digital de la señal Binary Frequency Shift Keying (BFSK). El objetivo de la investigación es en la obtención de un nuevo método de procesamiento para demodular señales BFSK, el cual presenta menos complejidad en hardware que los reportados hasta la fecha. El sistema propuesto hace uso de la teoría de filtros adaptados y de los algoritmos de segmentación de curvas. El artículo describe la integración y configuración de un bloque de correlador por muestreo con un bloque de segmentación de curvas con el objetivo de obtener un receptor digital para demodular apropiadamente la señal recibida. La solución propuesta reduce considerablemente la complejidad en hardware. En esta parte se expone el sistema abordando de forma analítica las expresiones que lo describen. El artículo aborda en detalle los elementos necesarios para la configuración del sistema. En una segunda parte se muestra la implementación del sistema en FPGA así como los resultados de simulación que validan el desempeño del sistema.

Palabras clave: Filtros adaptados, segmentación de curvas, demodulación digital, BFSK, FPGA.

Received: November 20th 2014
Accepted: July 22nd 2015

Introduction

Frequency Shift Keying (FSK) is a digital modulation format with applications in wireless technologies (Ibrahim et al., 2013) (Peng et al., 2013), satellite communications (VEŘTÁT, MRÁZ, 2013), power lines communications (PLC) (Ouahada, 2014), mobile communications (Karabulut, 2015), spread spectrum systems (Neifar, 2012) and biomedical applications (Wang, 2014). Various configurations of circuitry have previously been reported for BFSK demodulators. Some of them, especially those based on a correlator receiver model, are particularly interesting because they perform signal to noise ratio maximization (Sklar, 2001) and do not use symbol sychronization blocks, such as Quadricorrelator (Gardner, 1985), Balanced Quadricorrelator (Kang et al., 2011) and Quotient Detector (Kreuzgruber, 1994).

These types of detectors are implemented in a two-part structure The first part is an analogue correlator (Egau, 1984); the second part includes procedures for derivation,

[1] Jorge Torres Gómez: BSc. in Telecommunications and Electronics, MSc. in Telecommunication Systems, Affiliation: Department of Telecommunications and Telematics, Electrical School, CUJAE, Cuba.
E-mail: jorge.tg@electrica.cujae.edu.cu E-mail: jtorres151184@gmail.com

[2] Fidel Ernesto Hernández Montero: MSc in Digital Systems from CUJAE in 2000, PhD degree in Electronics and Industrial Automation from University of Mondragon, Spain, in 2006, Affiliation: Department of Telecommunications and Telematics, Electrical School, CUJAE, Cuba.
E-mail: fhernandez@electrica.cujae.edu.cu

[3] Joachim Habermann: Dr.-Ing. (PhD) degrees in Electrical Engineering both with highest honors from the Technical University of Darmstadt, Germany. Senior member of the Institute of Electrical and Electronics Engineers (SM IEEE). Reviewer of several research institutions, such as the Deutsche Forschungsgemeinschaft (DFG), Affiliation: full professor in the Department of Electrical Engineering and Information Technology of the Technische Hochschule Mittelhessen (THM), University of Applied Sciences Giessen, Germany.
E-mail: joachim.habermann@iem.thm.de

How to cite: Torres, J., Hernández, F., & Habermann, J. (2015). New digital demodulator with matched filters and curve segmentation techniques for BFSK demodulation: Analytical description. *Ingeniería e Investigación, 35(3)*, 92-99. DOI: http://dx.doi.org/10.15446/ing.investig.v35n3.47386

addition and multiplication, in order to extract the instantaneous frequency. Figure 1 depicts the block diagram of the Balanced Quadricorrelator. However, due to the large number of adders and multipliers needed for the lowpass filter (LPF) implementation, such digital implementations demand a high cost.

Although the low pass filter and the multiplication procedure could be obtained through a flip-flop element, as in the digital logic quadricorrelator scheme of (Ahn et al., 2005), and the differentiator can be accomplished by flip-flop blocks followed by AND-gates, this type of solution is prone to instabilities under conditions of low signal to noise ratio. This causes total interruption of the counting process at the system output, despite its low hardware consumption.

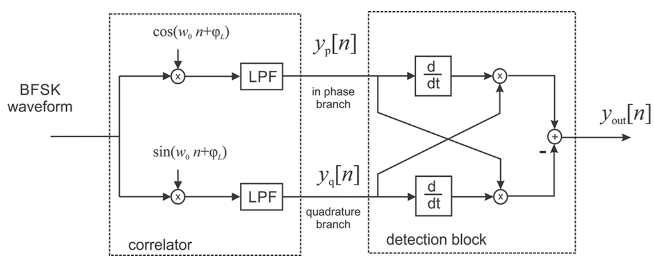

Figure 1. Block Scheme of the Balanced Quadricorrelator.

The method discussed in this paper outperforms all previous correlator-based schemes, in terms of hardware complexity. A new BFSK detection correlator-based scheme, directed to the slope recognition instead of the instantaneous frequency at the correlator output, is devised. This article addresses in detail the analytical expressions used to describe the proposed solution, which exhibit a strong reduction with regard to hardware complexity.

The rest of the paper is organized as follows: Section 2 summarizes the proposed solution in a descriptive way, for ease of exposition. Section 3 addresses the analytical expressions for configuring the proposed solution. Section 4 addresses a discussion with regard to hardware complexity. Finally, the Conclusions are presented in Section 5.

Receiver conception. Cualitative description.

In the scheme proposed in this paper a Discrete Correlator (Lee et al., 1950) is employed in order to reduce hardware complexity (the scheme is depicted in Figure 2). The correlator is configured with a local tone of frequency w_0 and phase φ_L. The received BFSK waveform arrives with a frequency w_i, i either 0 or 1, with phase φ_0 and amplitude given by A_c.

At the output of the sampler correlator, linear segments are obtained in the temporal series of $y_p[n]$ and $y_q[n]$ for the in phase and quadrature branches, respectively. The slope of these segments depends on the symbol received. For instance, considering the result shown in Figure 3, it can be noted that with the received lower frequency w_1 the output of the correlator is comprised by segments of zero slope (e.g. $\overline{AB}$ and $\overline{CD}$). On the other hand, with the received higher frequency w_0, the output is comprised by segments of non-zero slope (e.g. $\overline{BC}$).

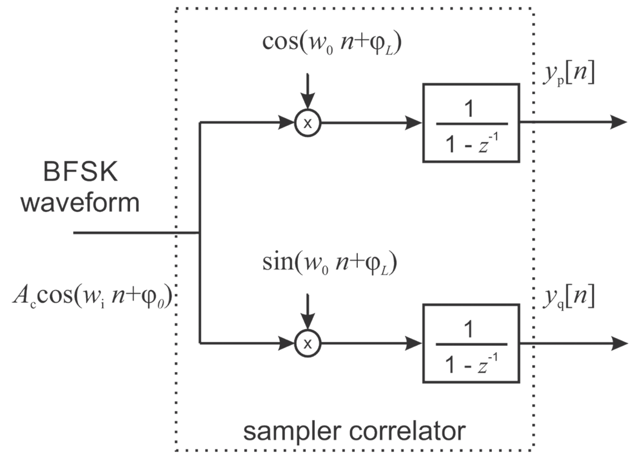

Figure 2. Receiver for the BFSK waveform with segmentation curve techniques.

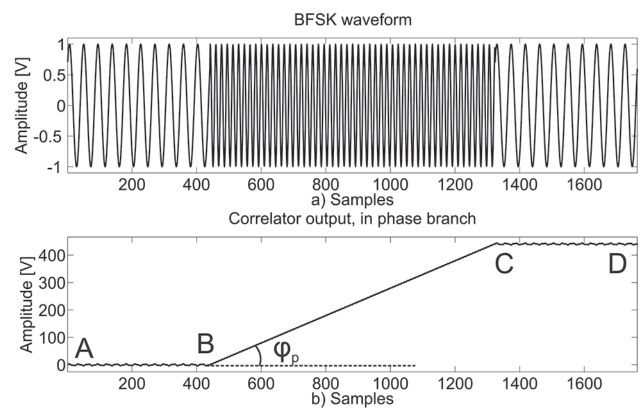

Figure 3. a) Waveform Received. b) Discrete Correlator output.

The main idea of the proposed receiver is to identify the approximate linear signal ramp observed at the output of the correlator for a sine-wave input (Sklar, 2001), and, by means of this procedure, to identify the symbols received. The change of slope in the curve showed in Figure 3b is directly related to the symbol transmitted. Therefore, methods for recognizing such changes can be employed for demodulation purposes.

The curve in Figure 3b is comprised by the linear segments $\overline{AB}$, $\overline{BC}$ and $\overline{CD}$, and the split of a curve into linear segments is a task intensively studied in the field of curve segmentation by means of two categories (Iñesta et al., 1998): feature point approach and error tolerance approach. This paper addresses those methods based on the feature point approach.

Methods of feature point approach identify dominant points, such as B and C, by means of a curvature measurement. Consequently, this measure can be directly related to the slope of each segment. The techniques of curve segmentation can be employed for extracting the *tanφ* of each segment on Figure 3b.

In average, the slope of segment $\overline{AB}$ is approximately zero, whereas the slope of segment $\overline{BC}$ can be described, for the in phase branch, as in (Sklar, 2001):

$$tan\varphi_p \;=\; \frac{A_c}{2}\; cos\left(\varphi_0 - \varphi_L\right) \tag{1}$$

For the quadrature branch a similar results is obtained:

$$tan\varphi_q \;=-\; \frac{A_c}{2}\; sin\left(\varphi_0 - \varphi_L\right) \tag{2}$$

Considering the values of the slope in Equations (1) and (2), a receiver can be implemented by squaring the tangent functions in Equations (1) and (2), which yields to:

$$y_{out}\left[n\right] = tan^2\varphi_p + tan^2\varphi_q = \begin{cases} \left(\dfrac{A_c}{2}\right)^2 & if \;\; w_i = w_0 \\ 0 & if \;\; w_i \neq w_0 \end{cases} \tag{3}$$

Summarizing, the proposed solution uses the sampler correlator of Figure 2 in order to obtain the linear curves, the slope that can be estimated by curve segmentation techniques. After estimating the slope values in Equations (1) and (2), the operation in Equation (3) is performed for obtaining high and low levels and then recovering the transmitted bits. The general scheme is depicted in Figure 4 and the output is depicted in Figure 5.

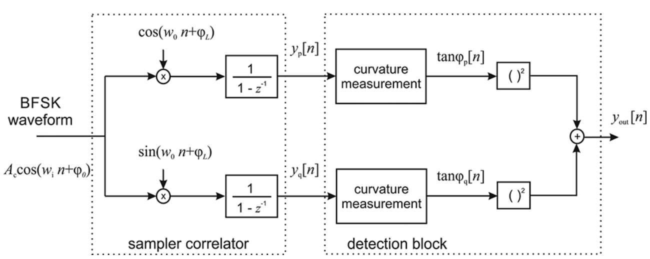

Figure 4. Receiver for the BFSK waveform with segmentation curve techniques.

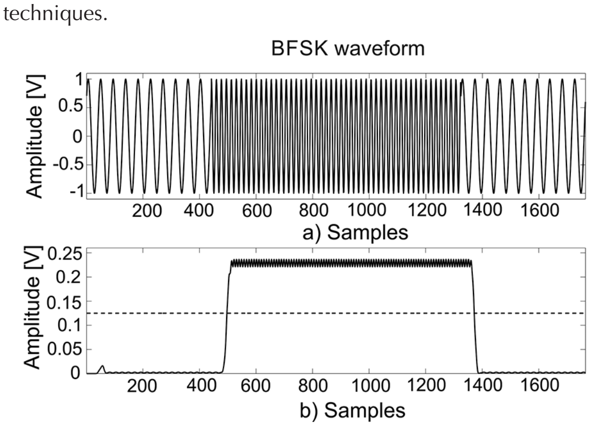

Figure 5. a) Upper part: Receiver input in Figure 3. b) Lower part: Output for the receiver in Figure 3 applying k-angular bending segmentation curve algorithm. Parameters: w_0=0,1425 rad/s, w_1=0,3562 rad/s, k=44 samples.

From Figure 5 it can be noted that the pulses in b) can be used to detect the frequency received in a); this detection can be accomplished by means of threshold (dotted line), the value that is determined in Section 3.

Curvature measurement methods

Once the signal of the sampler correlation output is obtained, the estimation of the slope of each segment follows. To that end, the use of curvature measurement methods is analyzed.

Methods such as k-cosine (Wang et al., 2010), k-angular bending (Iñesta et al., 1998), Distance Accumulator (Han, Poston, 1993) and Scatter Matrix (Anderson, Bezdek, 1984) are usually employed to measure the curvature from images. Among this methods, the k-angular bending is the only one that does not implement a division procedure for estimating the slope. This is an important issue concerning a practical implementation in hardware, for instance in FPGA, since a division procedure can produce undesirable glitches at the output. Therefore, the implementation of k-angular bending is considered here for implementing the block curvature measurement depicted in Figure 3.

k-angular bending foundations

This method estimates the slope for each segment calculating the ratio between the incoming values and the time index in a sliding window of length *k*. At the same time, an average procedure is also implemented for reducing the effect of noise. The value for *tanφ[n]*, for the quadrature and the in phase branches, is obtained through the following relation:

$$tan\varphi\left[n\right] = \frac{\overline{y_{bn}\left[n\right]} - \overline{y_{an}\left[n\right]}}{\overline{x_{bn}\left[n\right]} - \overline{x_{an}\left[n\right]}} \tag{4}$$

where:

$$\overline{y_{bn}\left[n\right]} = \left(k/2+1\right)^{-1}\sum_{i=n}^{n+k/2} y_i \qquad \overline{x_{bn}\left[n\right]} = \left(k/2+1\right)^{-1}\sum_{i=n}^{n+k/2} i$$

$$\overline{y_{an}\left[n\right]} = \left(k/2+1\right)^{-1}\sum_{i=n-k/2}^{n} y_i \qquad \overline{x_{an}\left[n\right]} = \left(k/2+1\right)^{-1}\sum_{i=n-k/2}^{n} i$$

y_l: samples of the curve

i: time index of the curve

k: length of the window

The average procedure is obtained with the previous definition of $\overline{y_{bn}\left[n\right]}$ and $\overline{y_{an}\left[n\right]}$. The expression given in Equation (4) can also be simplified as indicated by:

$$tan\varphi\left[n\right] = c\sum_{i=n}^{n+k/2}\left(y\left[i\right] - y\left[i-k/2\right]\right) \tag{5}$$

where:

$$c = \left(k/2\right)^{-1}\left(k/2+1\right)^{-1}$$

Considering the numerator in Equation (4), the expression can be simplified as:

$$\overline{y_{bn}[n]} - \overline{y_{an}[n]} = \left(k/2+1\right)^{-1} \sum_{i=n}^{n+k/2}\left(y[i]-y[i-k/2]\right) \quad (6)$$

Considering the denominator in Equation (4), the expression can be simplified by means of:

$$\overline{x_{bn}} - \overline{x_{an}} = \left(\frac{k}{2}+1\right)^{-1}\left(\sum_{i=n}^{n+\frac{k}{2}} i - \sum_{i=n-\frac{k}{2}}^{n} i\right) = \left(\frac{k}{2}+1\right)^{-1} 2\left(1+2+\cdots+\frac{k}{2}\right) = \left(k/2+1\right)^{-1} k/2\left(1+k/2\right) = k/2 \quad (7)$$

Then, when applying this procedure in the curvature measurement block of Figure 3, the output signal will be high or low, corresponding to the higher or lower frequency of the input signal, respectively (see Figure 4). Thus, changes in those levels can be employed for detecting the symbol transmitted. For this purpose, a proper threshold must be derived, which is addressed in the next Section. The expression given in Equation (6) is useful in the digital implementation of the system, an issue that will considered in the second part of this paper.

Receiver conception. Analytical description

in order to recover the bits transmitted, it is necessary to establish a threshold for identifying the high from the low levels at the output of the receiver. This is indicated by the dotted line in Figure 5b).

When the operation in Equation (3) is performed, additional oscillation is introduced around the expected values $\frac{A_c^2}{4}$ and 0, in the absence of noise. These oscillations are easily verified in the high level of Figure 4b they are produced by the multiplication of the received signal with the local tone. Besides, the amplitude of these oscillations depends on the levels at the output of the system, and this can be verified on Figure 4b. In this case, the high level exhibits an oscillating behavior with higher amplitude than the low level.

In order to establish a threshold, the oscillations produced by the operation given in Equation (3) must be considered. Taking into account that the amplitude of these oscillations depends on the binary levels, then the threshold is not easily established as the half of the maximum amplitude; it also depends on the oscillating terms. In order to obtain a proper value for the threshold, it is necessary to analytically describe the proposed system, and this is addressed by the following steps:

1. The obtaining of the analytical expressions for $y_p[n]$ and $y_q[n]$ of Figure 2.
2. The obtaining of the variance around the binary levels at the output of the system of Figure 4.

Analytical expression for $y_p[n]$ and $y_q[n]$

To obtain the analytical expressions, there are two cases to be described. The case in which the lower frequency is received, w_1, and the case of the higher frequency, w_0. For the latter, the output of the correlator is as follows (details are given in the Appendix A):

$$y_p[n] = \frac{A_c}{2} cos\left(\varphi_0 - \varphi_L\right)\left(n+1\right) + y^*_{p00}[n] \quad (8)$$

where:

$$y^*_{p00}[n] = \frac{A_c}{4\ sin\left(w_0\right)}\left(\begin{array}{l} sin\left(w_0-\varphi_0-\varphi_L\right) \\ +sin\left(\begin{array}{l} 2w_0\left(n+1/2\right) \\ +\varphi_0+\varphi_L \end{array}\right)\end{array}\right) \quad (9)$$

From Equation (8) it can be observed that the first term is directly related to the ramp signal, and this is described by the segment $\overline{BC}$ on Figure 3b). This segment has a maximum slope given by $\frac{A_c^2}{2}$, which means that the maximum voltage at the output of the correlator will be given by $\frac{A_c^2}{4}\left(N+1\right)$, where N represents the total number of samples between transitions. Thus, the system used to implement the receiver in Figure 4 should be capable of storing this value. Additionally, once the detection block identifies a transition, then a reset on the accumulator block can be settled. By this mechanism, the values of $y_p[n]$ and $y_q[n]$ will be set to zero in order to avoid larger values than $\frac{A_c^2}{2}\left(N+1\right)$.

The slope of is the segments in the phase and quadrature branches are the average value to be estimated by the k-bending method. On the other hand, there is also an oscillating term, denoted by $y^*_{p00}[n]$ in Equation (9), which produces the oscillating behavior at the output of the system. For the quadrature branch a similar description to Equation (8) is obtained, except that φ_L must be replaced by $\left(\varphi_L - \frac{\pi}{2}\right)$.

On the other hand, the analytical description when the received frequency is w_1 is given by the relation (A3) in the Appendix ,when $w_i = w_0$, and denoted by $y^*_{p10}[n]$. In this case, the slope is zero in average; this is graphically described by the segments $\overline{AB}$ and $\overline{CD}$ in Figure 3.

Variance at the output of the system.

The variance at the output of the system is given by the oscillating term $y^{*}_{p00}\left[n\right]$ for the high levels and $y^{*}_{p10}\left[n\right]$ for the low levels. The method of k-bending performs the sum indicated in Equation (6), which can be arranged in a different way for the ease of calculation as follows:

$$\overline{y^{*}_{bn}}[n]-\overline{y^{*}_{an}}[n]=(k/2+1)^{-1}\sum_{i=1}^{k/2}(y^{*}_{p00}[n+i]-y^{*}_{p00}[n-i]) \quad (10)$$

Taking into account the use of trigonometric identities for the subtraction of sine functions, the term $\left(y^{*}_{p00}\left[n+i\right]-y^{*}_{p00}\left[n-i\right]\right)$ can be simplified as:

$$\begin{aligned}\left(y^{*}_{p00}\left[n+i\right]-y^{*}_{p00}\left[n-i\right]\right)&=\frac{A_c}{4\ sin\left(w_0\right)}\left(sin\left(2w_0\left(n+i+1/2\right)+\varphi_0+\varphi_L\right)-sin\left(2w_0\left(n-i+1/2\right)+\varphi_0+\varphi_L\right)\right)\\&=\frac{A_c}{2\ sin\left(w_0\right)}sin\left(w_0 i\right)cos\left(2w_0\left(n+1/2+\varphi_0+\varphi_L\right)\right)\end{aligned} \quad (11)$$

An upper bound for Equation (11) can be obtained by:

$$\left(y^{*}_{p00}\left[n+i\right]-y^{*}_{p00}\left[n-i\right]\right)\leq\left|\frac{A_c}{2\ sin\left(w_0\right)}sin\left(w_0 i\right)\right| \quad (12)$$

According to the upper bound in Equation (12), which is independent of the time index n, the sum in Equation (10) can be upper bounded as follows:

$$\begin{aligned}&\sum_{i=1}^{\frac{k}{2}}\left(y^{*}_{p00}\left[n+i\right]-y^{*}_{p00}\left[n-i\right]\right)\leq\\&\left|\frac{A_c}{2\ sin\left(w_0\right)}\right|\sum_{i=1}^{\frac{k}{2}}\left|sin\left(w_0 i\right)\right|\\&\leq\left|\frac{A_c}{2\ sin^2\left(w_0\right)}sin\left(w_0\left(\frac{k}{2}+1\right)\right)sin\left(w_0\frac{k}{4}\right)\right|=\Delta_{p00}\end{aligned} \quad (13)$$

This sum formula is obtained by straightforward methods, described in Appendix B. The relation in Equation (13) is also valid for the quadrature branch, since the phase terms φ_0 and φ_L have been neglected; this is denoted by Δ_{q00}.

Finally, the variance of the output $y_{out}[n]$, for $w_1=w_0$, can be upper bounded by:

$$var_y\leq\left(c\ \ \Delta_{p00}\right)^2+\left(c\ \ \Delta_{q00}\right)^2 \quad (14)$$

The quantities given by Δ_{p00} and Δ_{q00} are equal in value, and they represent the maximum amplitude of the oscillations at the output of the square procedure for both branches in Figure 4. However, these oscillations are orthogonal, thus the sum in Equation (14) can be upper bounded as:

$$var_y\leq\left(c\ \ \Delta_{p00}\right)^2+\left(c\ \ \Delta_{q00}\right)^2\leq\sqrt{2}\ \left(c\ \ \Delta_{p00}\right)^2=\Delta_1 \quad (15)$$

given that the maximum value of the sum of a sine and a cosine function is $\sqrt{2}$.

Secondly, when $w_1\neq w_0$ the variance of the output $y_{out}[n]$ can be obtained by means of the procedure implemented for obtaining Equation (15). In this case, $y^{*}_{p10}\left[n\right]$ comprises two tones, one of them at the frequency $\frac{w_0+w_1}{2}$ and the other tone at $\frac{w_0-w_1}{2}$, as described in Equation (A3), in Appendix A. Similar to Equation (15), an upper bound can be obtained as:

$$\begin{aligned}&\sum_{j=1}^{\frac{k}{2}}\left(y^{*}_{p10}\left[n+i\right]-y^{*}_{p10}\left[n-i\right]\right)\leq\\&\leq\left|\frac{A_c}{2sin^2\left(\frac{w_0+w_1}{2}\right)}\sin\left(\frac{w_0+w_1}{2}\left(\frac{k}{2}+1\right)\right)sin\left(\frac{w_0+w_1}{2}\frac{k}{2}\right)\right|\\&+\left|\frac{A_c}{2sin^2\left(\frac{w_0-w_1}{2}\right)}\sin\left(\frac{w_0-w_1}{2}\left(\frac{k}{2}+1\right)\right)sin\left(\frac{w_0-w_1}{2}\frac{k}{2}\right)\right|\\&=\Delta_{p01}\end{aligned} \quad (16)$$

For the quadrature branch, a similar upper bound is obtained; this is denoted by Δ_{q01}. Finally, after squaring and multiplying by $\sqrt{2}\,c^2$, an upper bound is obtained by:

$$var_y\leq\left(c\ \ \Delta_{p01}\right)^2+\left(c\ \ \Delta_{q01}\right)^2\leq\sqrt{2}\ \left(c\ \ \Delta_{p01}\right)^2=\Delta_0 \quad (17)$$

Once the variances are obtained around the high and the low levels, a threshold can be established for detecting the transitions. In case of the high level, the amplitude of the oscillation is given by Δ_1 in Equation (15), with a direct component equal to $\frac{A_c^2}{4}$, as given in Equation (3).

For the low levels, the amplitude of the oscillation is given by Δ_0. As such, the threshold must be established in some intermediate point between $\left(\frac{A_c^2}{4}-\Delta_1\right)$ and Δ_0. Here the threshold is placed on the middle for increasing the margin noise as:

$$y_{th} = \frac{1}{2}\left(\frac{A_c^2}{4} - \Delta_1 + \Delta_0\right) \tag{18}$$

The threshold given in Equation (18) is employed to distinguish the low and high levels of the output signal; Figure 5 b) shows the result by means of dotted line with Δ_1=0,0637, Δ_0=0,0108, and y_{th}=0,1250. The terms Δ_1 and Δ_0 represent the effect of the oscillating terms. The use of this relation is affordable if the amplitude of the oscillations around the high and low levels are not comparable, that is, if $\frac{A_c^2}{4} - \Delta_1 > \Delta_0$. Otherwise, a lowpass filter can be employed at the output of the system to attenuate the amplitude of such oscillations. The precision in the determination of transitions, given by the threshold and the risetime of the pulses, is directly related to the total number of bits to be demodulated without errors, an issue that will be analyzed in Section 2.4.

Besides, the length of window k can be established for attenuating Δ_1 or Δ_0 in Equations (15) and (17). Depending on which oscillating term is the highest, k may be chosen in order to make zero the sine function.

In case that the value of A_C is unknown, the expression given in Equation (18) requires to estimate this value. This is due to the fact that the output of the system is comprised by high and low levels. However, these levels can be transformed into bipolar pulses if the direct component (DC level) of the output sequence $y_p[n]$ is supressed. This can be achieved through the use of a Notch filter, the transfer function given by (Proakis, Manolakis, 2006):

$$H_{notch}(z) = \frac{1 - 2\cos(w_c)z^{-1} + z^{-2}}{1 - (1 + r^2)\cos(w_c)z^{-1} + r^2 z^{-2}} \tag{19}$$

where r and w_c represent the radius of the pole and the center frequency of the filter, respectively. In order to suppress the DC level, the value of w_c must be settled to zero. In this case, the expected value will be zero and the threshold can be settled to $y_{th}=0$.

Discussion

With regard to hardware complexity, the proposed scheme, with the description given in Figures 4, needs 7 adders and multipliers. Three adders comes from the accumulator blocks and the output of the system, two multipliers are from the squaring devices and the others two from the multiplier at the beginning of each branch. In addition, the curvature measurement blocks can be implemented with 2 FIR filters by means of a moving average structure (Oppenheim et al., 2010) without multipliers, since all the coefficients are equals to 1 as indicated in 5. Finally, through the use of the notch filter in Equation (21) a total of 7 adders and multipliers are also needed if the value of A_c is unknown.

On the other hand, considering the system for the Balanced Quadricorrelator in Figure 1, a total of 7 adders and multipliers with another 4 FIR filters are required. Comparing the elements needed for each receiver, the proposed solution may need 7 additional adders and multipliers, but a reduction of FIR filters is achieved. Furthermore, the FIR filters employed do not use multipliers and the order of the filters employed in the Balanced Quadricorrelator could be superior to that of the proposed system, taking into account the difference between w_0 and w_1.

Conclusions

The solution presented in this paper proposes a new detection scheme for demodulating BFSK signals. High-order filters are avoided because of one important matter: the symbol detection is accomplished through the constant slope recognition carried out at the output of a Sampler Correlator. This element represents the bridge between digital demodulation and curve segmentation techniques. From this point of view, new digital demodulators for BFSK waveforms can be developed, which advantageously save receiver complexity, in comparison to others reported. The system is only implemented by FIR and IIR filters, devices suitable to be implemented with low complexity.

Appendix A

This Section summarizes the obtaining of the analytical expressions for $y_p[n]$ and $y_q[n]$ in Figure 2. Considering the multiplication of the received signal by the local tone and after applying some trigonometric identities, the following expression is obtained:

$$\begin{aligned} &A_c\cos(w_i n + \varphi_0)\cdot\cos(w_0 n + \varphi_L) \\ &= \frac{A_c}{2}\begin{pmatrix} \cos(\varphi_0 - \varphi_L)x_1[n] - \sin(\varphi_0 - \varphi_L) \\ x_2[n] + \cos(\varphi_0 + \varphi_L)x_3[n] \\ -\sin(\varphi_0 + \varphi_L)x_4[n] \end{pmatrix} \end{aligned} \tag{A1}$$

Where:

$$x_1[n] = cos((w_i - w_0)n) \qquad x_3[n] = cos((w_i + w_0)n)$$

$$x_2[n] = sin((w_i - w_0)n) \qquad x_4[n] = sin((w_i + w_0)n)$$

The operation of the accumulator block from the sampler correlator is to perform the following sum:

$$\begin{aligned} &y_p[n] = \sum_{i=0}^{n} A_c\cos(w_i n + \varphi_0)\cdot\cos(w_0 n + \varphi_L) = \\ &\frac{A_c}{2}\begin{pmatrix} \cos(\varphi_0 - \varphi_L)\sum_{i=0}^{n} x_1[n] \\ -\sin(\varphi_0 - \varphi_L)\sum_{i=0}^{n} x_2[n] + \cos(\varphi_0 + \varphi_L)\sum_{i=0}^{n} x_3[n] \\ -\sin(\varphi_0 + \varphi_L)\sum_{i=0}^{n} x_4[n] \end{pmatrix} \end{aligned} \tag{A2}$$

After considering the Euler's theorem and the sum formula of the geometric progression (Gradshteyn 1980), it is possible to obtain closed form expressions for each term $\sum_{i=0}^{n} x_j[n]$ in Equation (A2). After some straightforward manipulations, the description for *yp [n]* yields:

$$y_p[n]=\frac{A_c}{2}+\frac{1}{sin\left(\frac{w_i+w_0}{2}\right)}sin\left(\frac{w_i+w_0}{2}(n+1)\right)cos\left(\frac{w_i+w_0}{2}n+\varphi_0-\varphi_L\right)\Bigg|+\frac{1}{sin\left(\frac{w_i+w_0}{2}\right)}sin\left(\frac{w_i+w_0}{2}(n+1)\right)cos\left(\frac{w_i+w_0}{2}n+\varphi_0-\varphi_L\right)\Bigg) \tag{A3}$$

The description given in Equation (A3) considers the case when the frequency received is different to that of the local tone, that is $w_1 \neq w_0$. The case in which $w_1=w_0$ can be obtained by taking the limit $\lim_{w_i\to w_0} y_p[n]$ to yield the relation:

$$y_p[n]=\frac{A_c}{2}cos(\varphi_0-\varphi_L)(n+1)+y^*_{p00}[n] \tag{A4}$$

where:

$$y^*_{p00}[n]=\frac{A_c}{4\ sin(w_0)}\Big(sin(w_0-\varphi_0-\varphi_L)+sin\big(2w_0(n+1/2)+\varphi_0+\varphi_L\big)\Big) \tag{A5}$$

For the quadrature branch similar expressions are obtained upon substituting φ_L by $\left(\varphi_L-\frac{\pi}{2}\right)$.

Appendix B

In this section the sum formula for relation Equation (13) is obtained as follows:

$$\sum_{i=1}^{\frac{k}{2}}\left|sin(w_0 i)\right|=\sum_{i=1}^{\frac{k}{2}}\left|\frac{e^{jw_0 i}-e^{-jw_0 i}}{2j}\right|\leq\left|\frac{\sum_{i=0}^{\frac{k}{2}}e^{jw_0 i}-\sum_{i=0}^{\frac{k}{2}}e^{-jw_0 i}}{2j}\right|=\left|\frac{\frac{1-e^{jw_0\left(\frac{k}{2}+1\right)}}{1-e^{jw_0}}-\frac{1-e^{-jw_0\left(\frac{k}{2}+1\right)}}{1-e^{-jw_0}}}{2j}\right|$$

$$=\left|\frac{1}{2j}\left(\frac{sin\left(\frac{w_0}{2}\left(\frac{k}{2}+1\right)\right)}{sin\left(\frac{w_0}{2}\right)}\frac{e^{j\frac{w_0}{2}\left(\frac{k}{2}+1\right)}}{e^{j\frac{w_0}{2}}}-\frac{sin\left(\frac{w_0}{2}\left(\frac{k}{2}+1\right)\right)}{sin\left(\frac{w_0}{2}\right)}\frac{e^{-j\frac{w_0}{2}\left(\frac{k}{2}+1\right)}}{e^{-j\frac{w_0}{2}}}\right)\right| \tag{B1}$$

$$=\left|\frac{sin\left(\frac{w_0}{2}\left(\frac{k}{2}+1\right)\right)}{sin\left(\frac{w_0}{2}\right)}\frac{1}{2j}\left(e^{j\frac{w_0}{2}\frac{k}{2}}-e^{-j\frac{w_0}{2}\frac{k}{2}}\right)\right|=\left|\frac{sin\left(\frac{w_0}{2}\left(\frac{k}{2}+1\right)\right)}{sin\left(\frac{w_0}{2}\right)}sin\left(w_0\frac{k}{4}\right)\right|$$

In this development, the Euler's identity and the formula of the geometric progression have been used (Gradshteyn 1980).

References

Ibrahim, G. H., Hafez, A., & Khalil, A. H. (2013). An ultra low power QPSK receiver based on super-regenerative oscillator with a novel digital phase detection technique. AEU - International Journal of Electronics and Communications, 67(11), 967–974. DOI: 10.1016/j.aeue.2013.05.008

Ouahada, K. (2014). Nonbinary convolutional codes and modified M-FSK detectors for power-line communications channel. Journal of Communications and Networks, 16(3), 270–279. DOI: 10.1109/JCN.2014.000047

Karabulut, M. A., Ozdemir, O., & Ilhan, H. (2015). Link adaptive relaying with noncoherent BFSK and DPSK modulations in multiple access relay channels. In Wireless Telecommunications Symposium (WTS), 2015 (pp. 1–5). DOI: 10.1109/WTS.2015.7117265

Neifar, A., Trabelsi, H., Bouzid, G., & Masmoudi, M. (2012). Design of a zero crossing BFSK demodulator for a wireless sensor. In 2012 7th International Conference on Design Technology of Integrated Systems in Nanoscale Era (DTIS) (pp. 1–5).

Wang, L.-H., Chen, T.-Y., Lin, K.-H., & Lee, S.-Y. (2014). A low-power super-regenerative BFSK transceiver for intelligent healthcare monitoring system. In 2014 IEEE International Symposium on Bioelectronics and Bioinformatics (ISBB) (pp. 1–4). DOI: 10.1109/ISBB.2014.6820913

Peng, K.-C., Lin, C.-C., & Chao, C.-H. (2013). A Novel Three-Point Modulation Technique for Fractional-N Frequency Synthesizer Applications. Radioengineering, 22(1), 269–275.

VEŘTÁT, I., & MRÁZ, J. (2013). Hybrid M-FSK/DQPSK Modulations for CubeSat Picosatellites. Radioengineering, 22(1), 389–393.

Sklar, B. (2001). Digital Communications, Fundamentals and Applications (Second). New Jersey: Prentice Hall.

Gardner, F. (1985). Properties of Frequency Difference Detectors. IEEE Transactions on Communications, 33(2), 131 – 138. DOI: 10.1109/TCOM.1985.1096264

Kang, H.-S., Kim, D., & Park, S.-C. (2011). Coarse frequency offset estimation using a delayed auto-quadricorrelator in OFDM-based WLANs. In 2011 3rd International Congress on Ultra Modern Telecommunications and Control Systems and Workshops (ICUMT) (pp. 1–4). Budapest, Hungary.

Kreuzgruber, P. (1994). A class of binary FSK direct conversion receivers. In Vehicular Technology Conference, 1994 IEEE 44th (pp. 457 –461 vol.1). DOI: 10.1109/vetec.1994.345086

Egau, P. C. (1984). Correlation systems in radio astronomy and related fields. Communications, Radar and Signal Processing, IEE Proceedings F, 131(1), 32 –39. DOI: 10.1049/ip-f-1.1984.0007

Ahn, T., Yoon, C.-G., & Moon, Y. (2005). An adaptive frequency calibration technique for fast locking wideband frequency synthesizers. In 48th Midwest Symposium on Circuits and Systems, 2005 (pp. 1899 –1902 Vol. 2). Cincinnati, Ohio, USA.

Lee, Y. W., Cheatham, T.P., J., & Wiesner, J. B. (1950). Application of Correlation Analysis to the Detection of Periodic Signals in Noise. Proceedings of the IRE, 38(10), 1165 – 1171. DOI: 10.1109/JRPROC.1950.233423

Iñesta, J. M., Buendí, M., & Sarti, M. Á. (1998). Reliable polygonal approximations of imaged real objects through dominant point detection. Pattern Recognition, 31(6), 685 – 697. DOI: 10.1016/S0031-3203(97)00081-2

Wang, C., Sun, G., Wang, Y., & Xu, L. (2010). An Improved Corner Detection Algorithm Based on Gaussian Smoothing. In 2010 International Conference on Intelligent Computation Technology and Automation (ICICTA) (Vol. 1, pp. 536–539). DOI: 10.1109/ICICTA.2010.449

Han, J. H., & Poston, T. (1993). Distance accumulation and planar curvature. In , Fourth International Conference on Computer Vision, 1993. Proceedings (pp. 487–491). DOI: 10.1109/ICCV.1993.378175

Anderson, I. M., & Bezdek, J. C. (1984). Curvature and Tangential Deflection of Discrete Arcs: A Theory Based on the Commutator of Scatter Matrix Pairs and Its Application to Vertex Detection in Planar Shape Data. IEEE Transactions on Pattern Analysis and Machine Intelligence, PAMI-6(1), 27–40. DOI: 10.1109/TPAMI.1984.4767472

Oppenheim, A. V., & Schafer, R. W. (2010). Discrete-time signal processing (Third Edition). Upper Saddle River, NJ, USA: Prentice Hall.

Gradshteyn, I. S., & Ryzhik, I. M. (1980). Table of Integrals, Series, and Products (fourth edition). Academic Press.

Kay, S. M. (1998). Fundamentals of Statistical Signal Processing: Estimation Theory (Vols. 1–3). Englewood Cliffs: Prentice-Hall.

Proakis, J. G., & Manolakis, D. G. (2006). Digital Signal Processing (Auflage: 4). Upper Saddle River, N.J: Prentice Hall.